Electronic Supplementary Material (ESI) for Journal of Materials Chemistry A.
This journal is © The Royal Society of Chemistry 2019

Carbon nanotubes confined iron modified cathode with prominent stability and activity for heterogeneous electro-Fenton

Pei Su[a,b,c,d], Minghua Zhou [a,b,c,d] *, Gengbo Ren[a,b,c,d], Xiaoye Lu[a,b,c,d], Xuedong Du[a,b,c,d], Ge Song[a,b,c,d]

[a] *Key Laboratory of Pollution Process and Environmental Criteria, Ministry of Education, College of Environmental Science and Engineering, Nankai University, Tianjin 300350, China.*

[b] *Tianjin Key Laboratory of Environmental Technology for Complex Trans-Media Pollution, Nankai University, Tianjin 300350, China*

[c] *Tianjin Key Laboratory of Urban Ecology Environmental Remediation and Pollution Control, College of Environmental Science and Engineering, Nankai University, Tianjin 300350, China*

[d] *Tianjin Advanced Water Treatment Technology International Joint Research Center, College of Environmental Science and Engineering, Nankai University, Tianjin 300350, China*

---

* Corresponding author. Tel/Fax: +86 022 23501117. E-mail address: zhoumh@nankai.edu.cn (M. Zhou).

Analytical methods

H_2O_2 measurement: At time intervals, 0.5 mL samples were taken for analyzing. And 0.5 mL potassium titanium (IV) oxalate solution (0.05 mol/L) and 0.5 ml H_2SO_4 (3 mol/L) were added into samples to analyze absorbance at λ=400 nm with the UV-vis spectrophotometer (UV759).

Total iron measurement: At time intervals, 1 mL samples were taken for analyzing the iron concentration. And 0.5 mL buffer solution (HAc-NaAc buffer solution, pH=4.6), 0.25 ml hydroxylamine hydrochloride (ω=1.0%) and 0.5 mL 1,10-phenanthroline monohydrat (ω=0.1%) were added into samples to analyze absorbance at λ=510 nm with the UV-vis spectrophotometer.

Hydroxyl radicals measurement ($^{\bullet}OH$): For the quantitative determination of $^{\bullet}OH$, dimethyl sulfoxide (DMSO, 0.2%) was first trapped in solution. And 1 mL samples were taken for analyzing. 2, 4-dinitrophenylhydrazine (DNPH, 0.2 mL), and phosphate buffer solutions (pH=4, 1.25 mL) were added into samples to form the corresponding hydrazine (HCHO-DNPH), which was determined by high performance liquid chromatography (Ultimate 3000, ThermoFisher, America) equipped with a BEH C18 column at a flow rate of 0.1 mL/min (1.7 μm, ϕ 2.1×100 mm). The mobile phase was methanol/water (% V/V = 60: 40) and 355 nm was chosen for detection.

Pollutants removal measurement: The experiments of phenol removal were performed at current of 60 mA. 0.5 mL sample was taken to analyze pollutants removal a time intervals. It was determined by same HPLC equipped with C18 column (3 μm, ϕ3.0×100 mm) and DAD detector at 0.3 mL/min. The mobile phase was methanol/water/glacial acetic acid (% V/V/V = 30: 19: 1) and 280 nm was chosen for detection.

Electric energy consumption (EEC) could be calculated by the following formula:[1]

$$\mathrm{EEC} = \frac{1000\mathrm{UIt}}{\mathrm{CV_s}} \qquad (1)$$

Where U is the voltage (V), I is the current (A), t is the time (h), V_s is the bulk volume (L), and C is the concentration of H_2O_2 (mg/L).

Exchange current density:

The exchange current density (i_0) was calculated from the Tafel equation: [1]

$$\lg(\frac{i}{i_0}) = \frac{\beta F\eta}{2.303RT} \quad (2)$$

Where η is the cathodic overpotential (V), R is the ideal gas constant (8.31 J/mol•K), T is the absolute temperature (K), β is the symmetry factor (a constant), F is the Faraday constant (96485 C/mol), i is the current density (mA/m^2) and i_0 is the exchange current density (mA/m^2). The linear Tafel regression ($R^2 \geq 0.99$) exists in the overpotential interval of 80 and 100 mV.

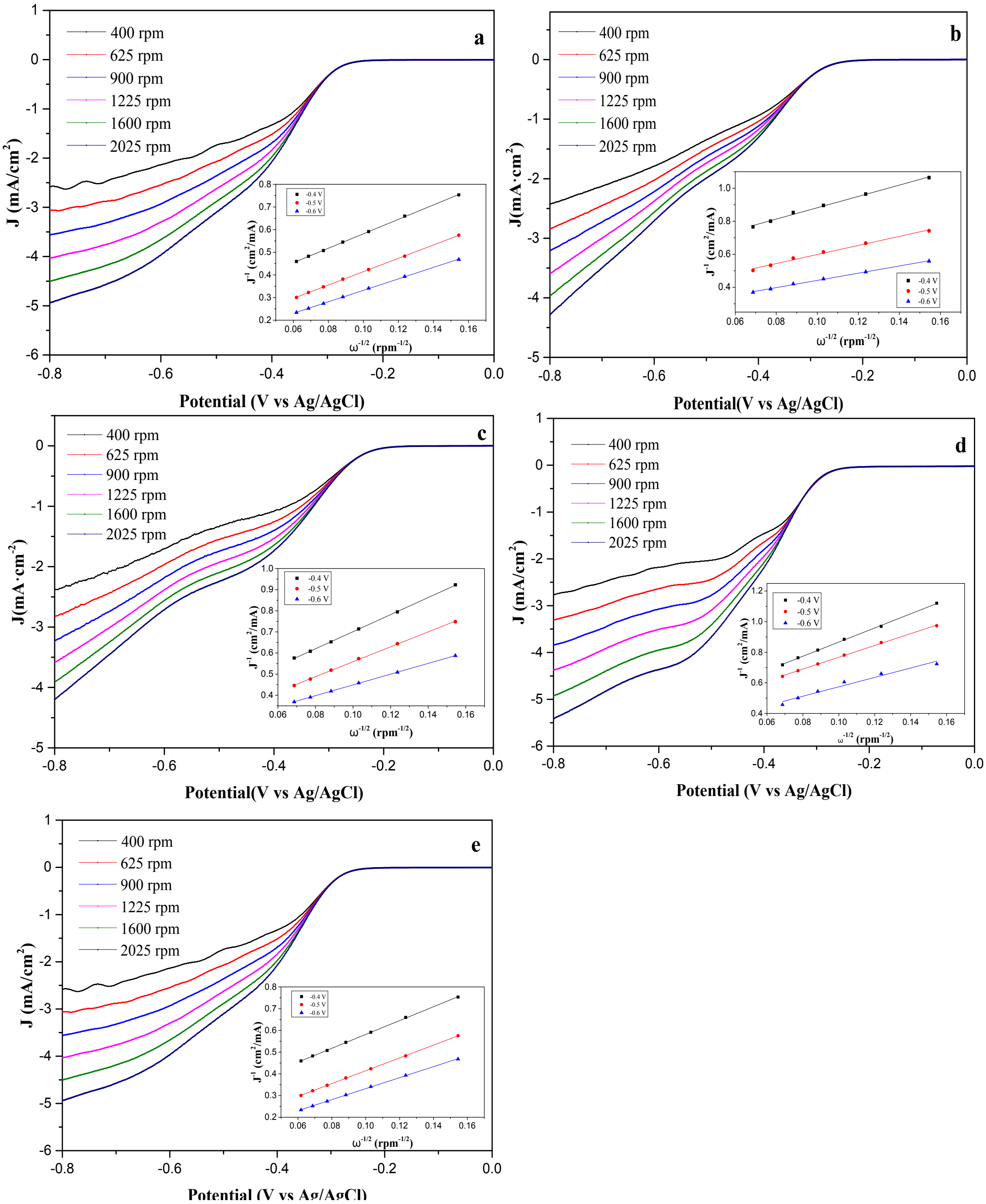

Figure S1 LSV by RDE for CNTs, Fe-in/out-CNTs, and Fe^0-in/out-CNTs (a-e)

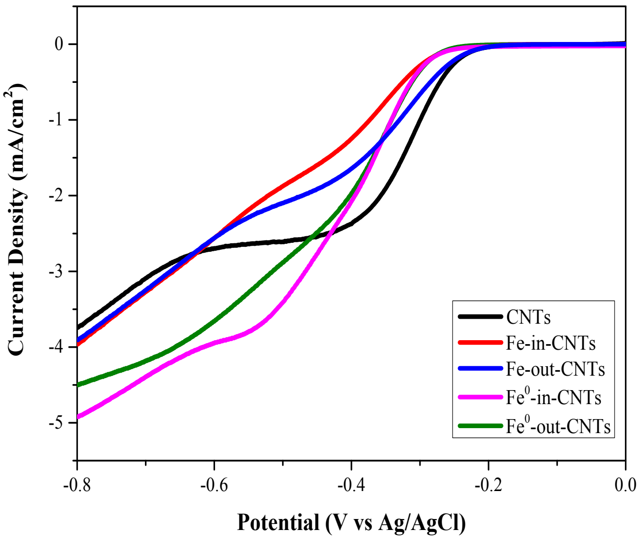

Figure S2 LSV at 1600 rpm for CNTs, Fe-in/out-CNTs, Fe^0-in/out-CNTs

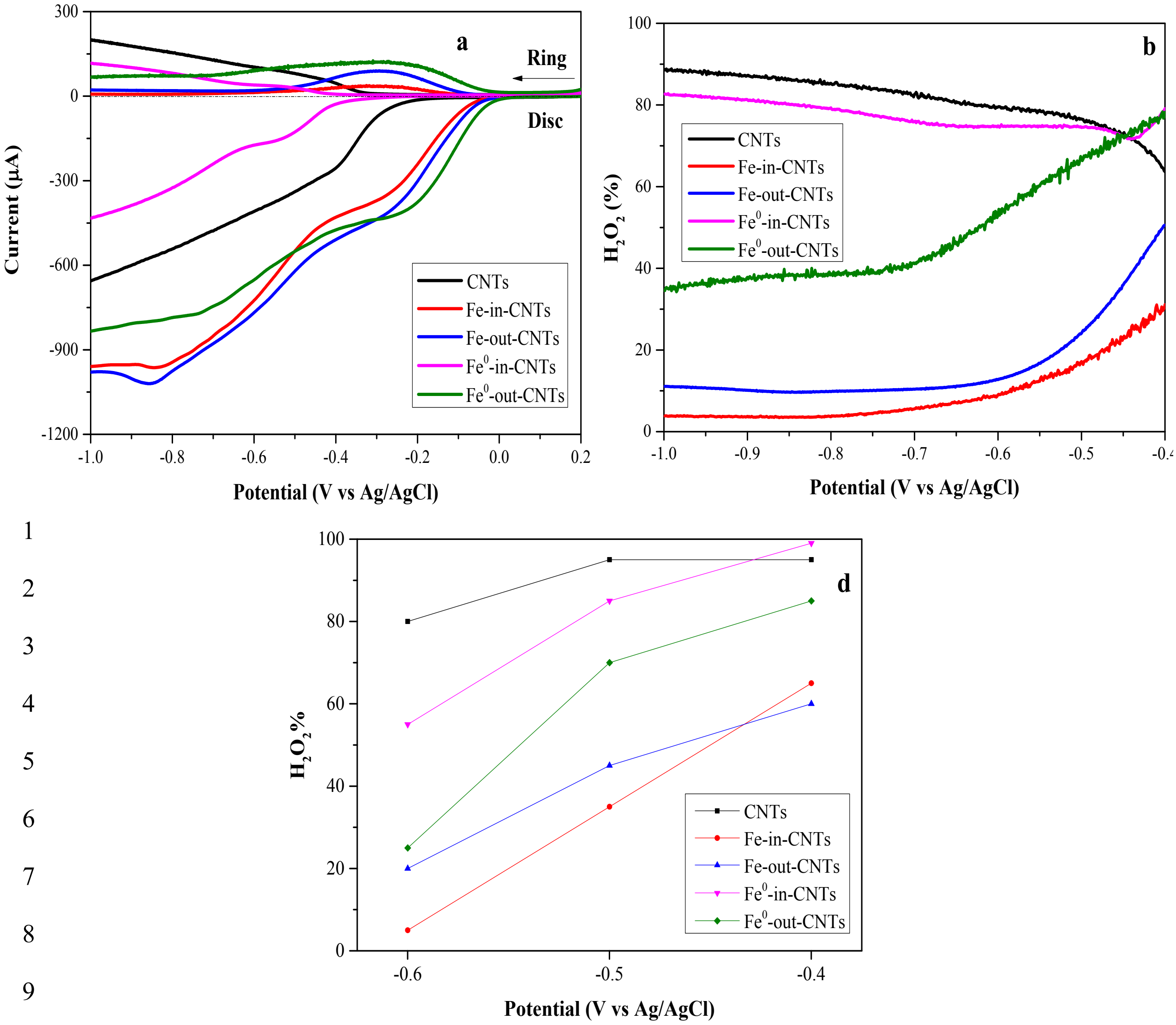

Figure S3 Disk current and ring current of RRDE tests at 1600 rpm (` **c** H_2O_2 selectivity from RRDE (b) and H_2O_2 selectivity from RDE (c) of CNTs, Fe-in/out-CNTs, and Fe^0-in/out-CNTs.

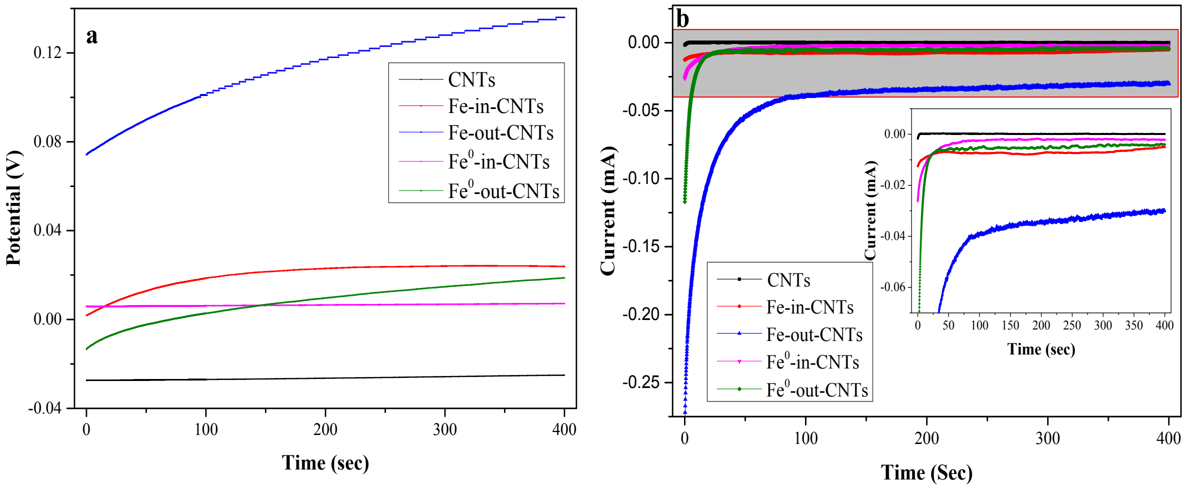

Figure S4 Stability tests of potential (a) and current (b) of CNTs, Fe-in/out-CNTs, and Fe^0-in/out-CNTs GDE

.

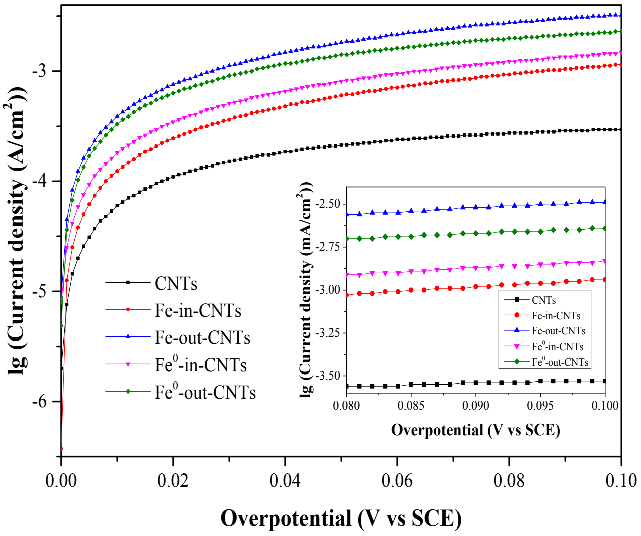

Figure S5 Tafel plots of CNTs, Fe-in/out-CNTs, and Fe^0-in/out-CNTs GDE

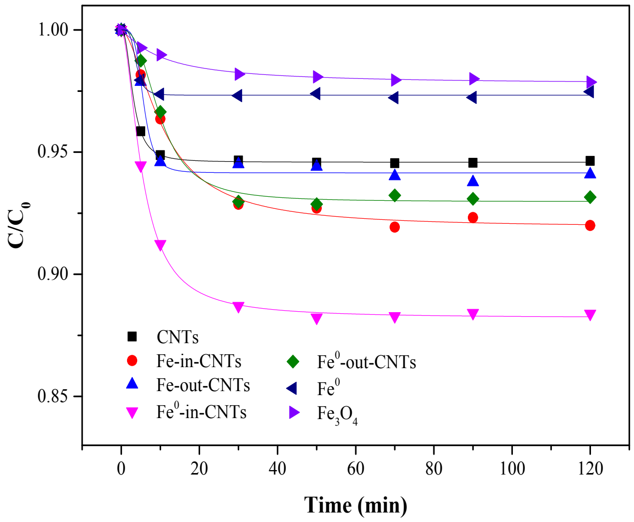

Figure S6 Phenol removal by different catalyst powder without H_2O_2

Conditions: pH=3, [catalyst]=0.1 g/L, [Phenol]=50 mg/L

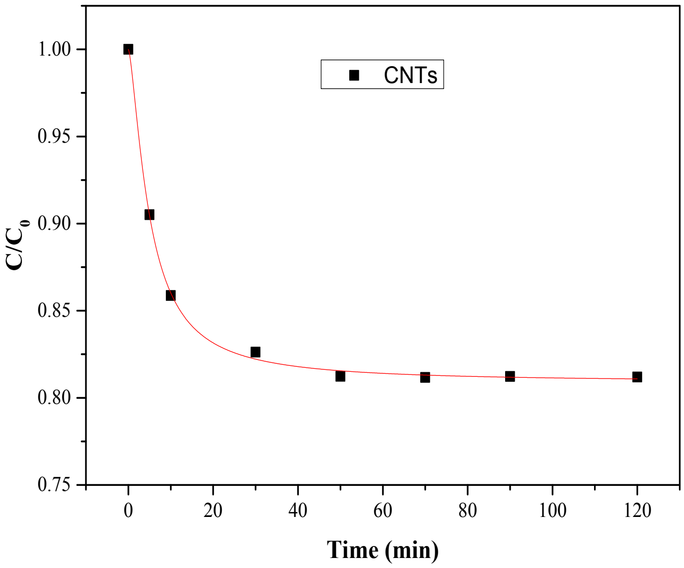

Figure S7 Phenol removal by CNT modified GDE when H_2O_2 was electro-synthesized

Conditions: V=300 ml, pH=3, I=60 mA, V_{air}=0.4 L/min, [Phenol]=50 mg/L

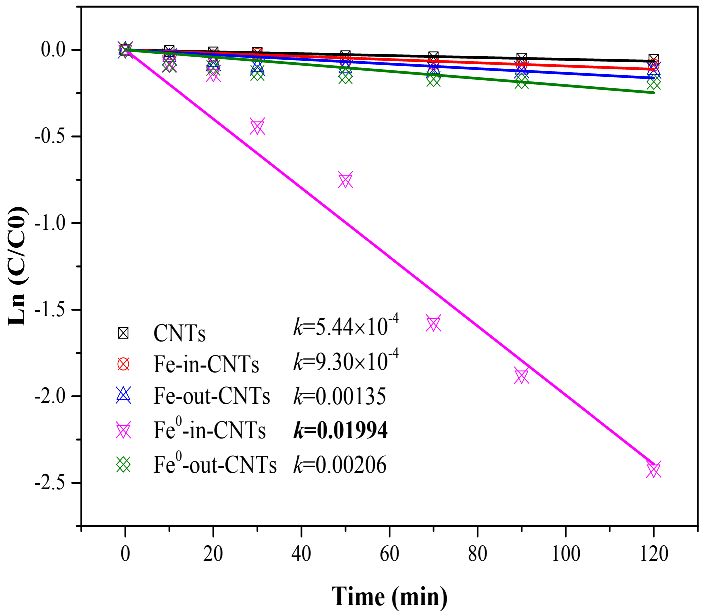

Figure S8 Pseudo-first-order constant (*k*) of phenol degradation by CNTs, Fe-in/out-CNTs and Fe^0-in/out-CNTs GDE

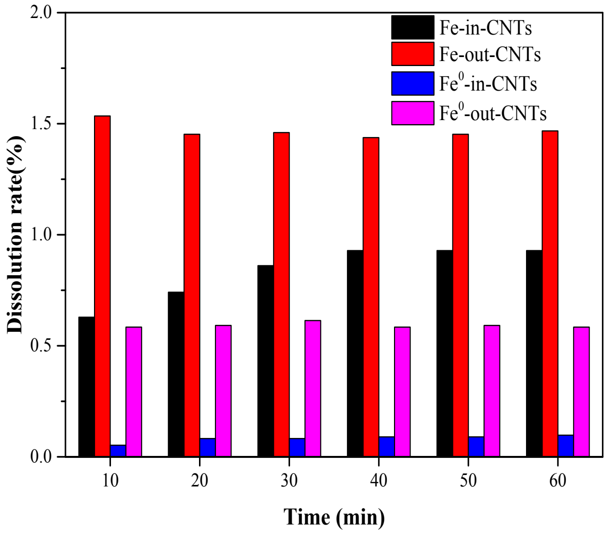

Figure S9 Iron dissolution rate of Fe-in/out-CNTs and Fe^0-in/out-CNTs GDE.

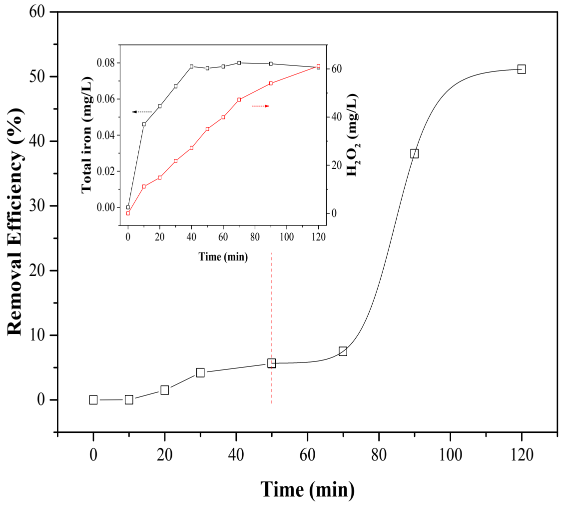

Figure S10 Phenol removal efficiency of Fe^0-in-CNTs GDE at neutral condition.

Condition: V=300 ml; pH=7; I=60 mA; V_{air}=0.4 L/min; phenol concentration: 50 mg/L

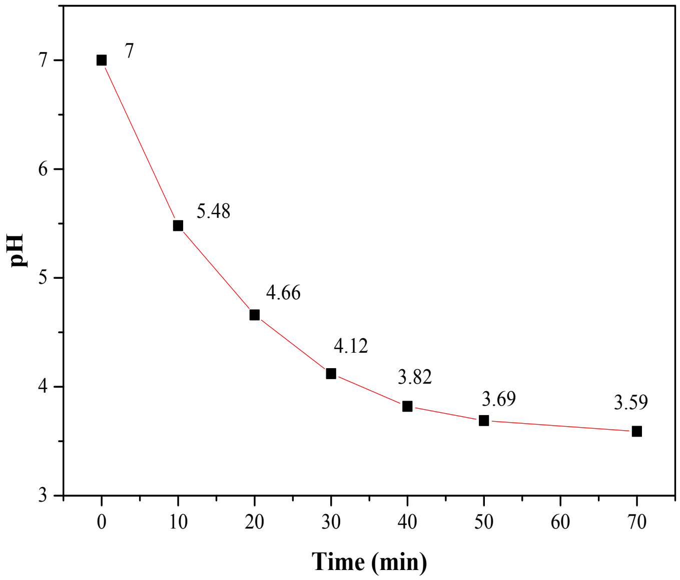

Figure S11 pH change when phenol was removed at neutral condition by Fe^0-in-CNTs GDE.

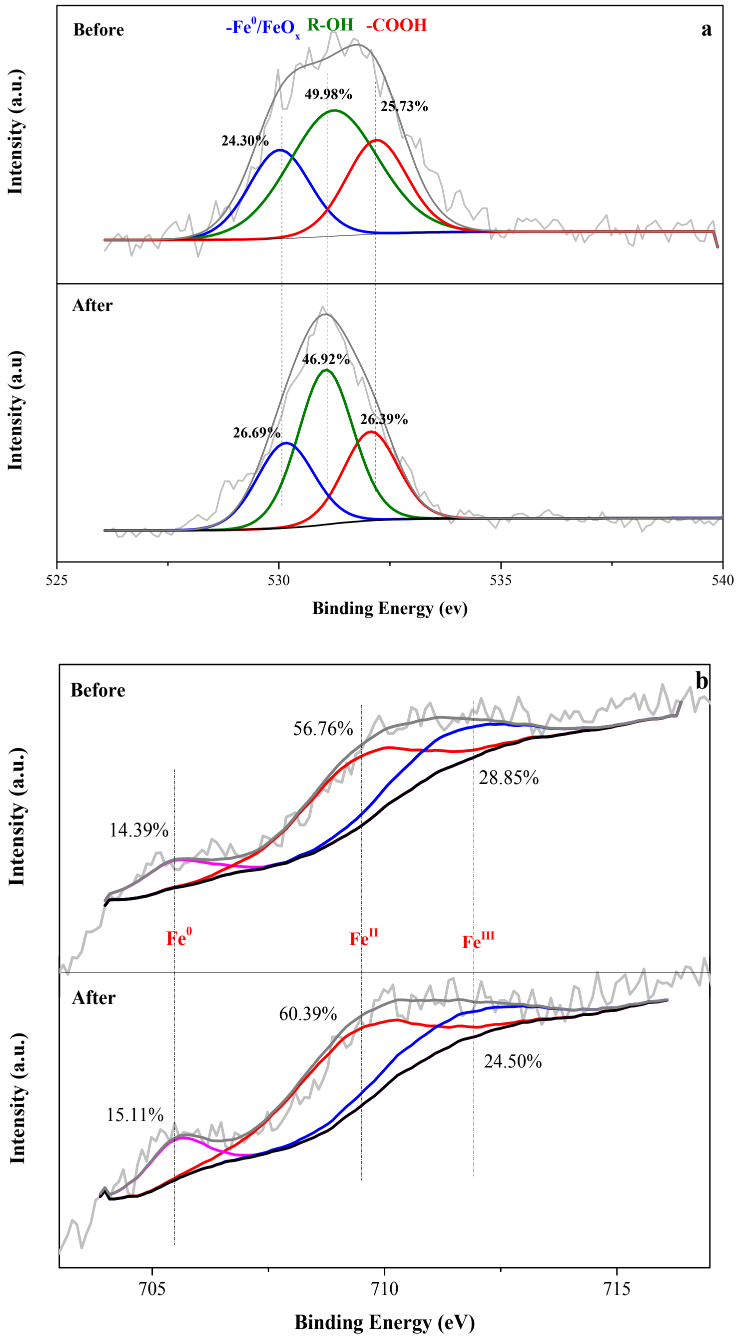

Figure S12 O1s (a) and Fe 2p (b) XPS spectra of the fresh and used Fe^0-out-CNTs GDE.

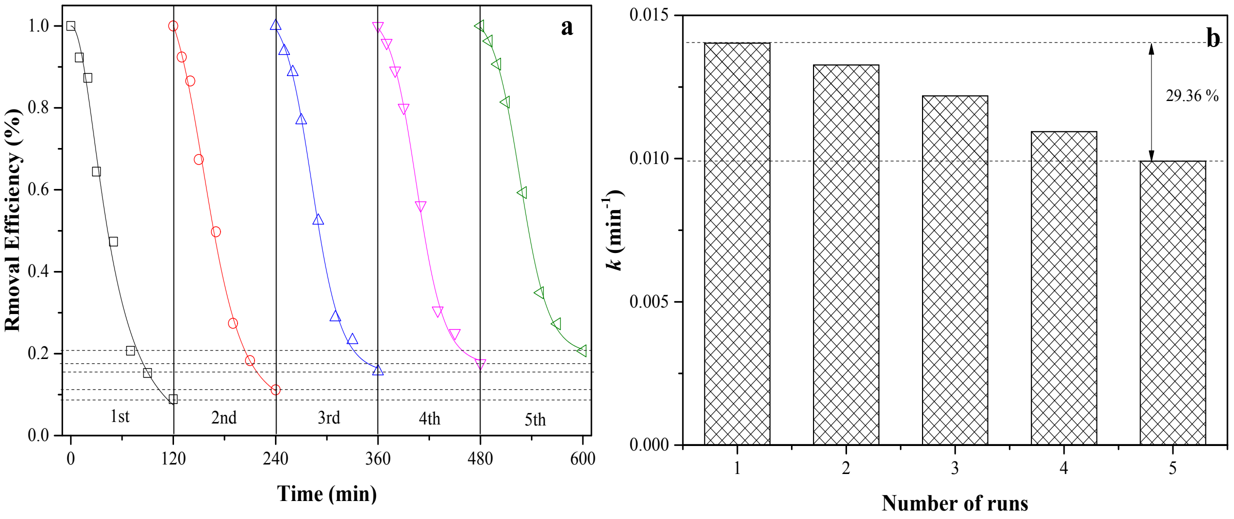

Figure S13 Stability of the Fe^0-in-CNTs GDE in the heterogeneous EF process over 5 cycles for the (a) phenol removal and (b) rate constant.

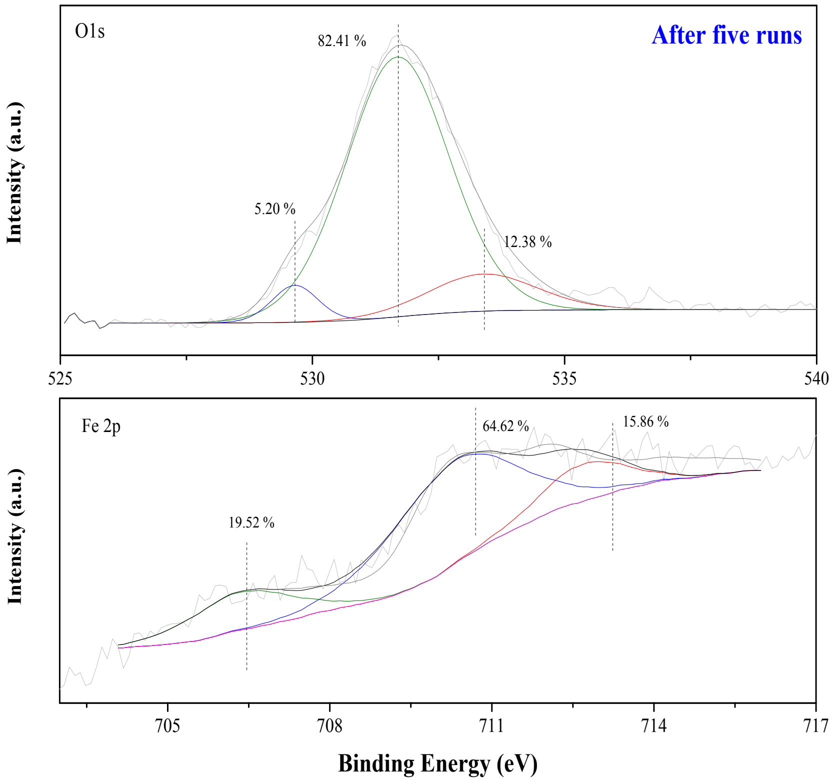

Figure S14 O1s and Fe 2p XPS spectra of Fe^0-in-CNTs GDE after five runs

Table S1 Electrochemical parameters for the ORR, EIS and polarization curve

	ORR		EIS			Tafel			
Materials	Reduction peaks (V vs Ag/AgCl)	Current density (mA/cm^2, -0.8 V) at 1600 rpm	R_0 (Ω)	Rct (Ω)	R_d (Ω)	E_{corr} (mV)	i_{corr} (mA/cm^2)	C_R (mm/a)	i_0 (A/cm^2)
CNTs	-0.419	3.74	9.13	8.37	11.79	-	-	-	8.8×10^{-3}
Fe-in-CNTs	-0.459	3.96	6.04	3.45	48.58	-144	0.247	2.86	0.18
Fe-out-CNTs	-0.376	4.50	6.10	3.59	38.08	-52	0.525	6.09	0.17
Fe^0-in-CNTs	-0.432	4.92	5.95	1.57	8.27	-189	0.170	1.97	0.15
Fe^0-out-CNTs	-0.391	3.90	6.33	3.06	10.70	-182	0.501	5.81	0.11

Cathode material	Experimental Conditions	Iron leaching mass (mg/cm^2, $\times 10^{-3}$)	EEC (kWh/kg $_{H2O2}$)	Pollutant Removal	Ref.
Fe@Fe_2O_3/active carbon fiber	Anode: BDD; pH=3; I=30 mA; t=60 min	18.2	-	(30 mg/L Atrazine) 100 %	2
Fe@Fe_2O_3/active carbon fiber	Anode: Bi_2WO_6/FTO electrode; pH=6.2; Light source=300 W; V_{air}=5 L/min; I=0.3 mA;t=120 min;	60.0	-	(1.0×10^{-5} M Rhodamine B) 46.9 %	3
Fe_3O_4/gas diffusion cathode	Anode: Pt sheet; pH=3 Cathode potential=-0.8 V; t=100 min;	460	-	(50 mg/L Tetracycline) 94.2 %	4
Fe_3O_4@Fe_2O_3/activated carbon aerogel	Anode: BDD; pH=3; Current density=10mA/cm^2; t=30 min; Pure oxygen=0.02m^3/h;	180	-	(236.7 mg/L Imidacloprid) 90 %	5
FeCu/Carbon aerogel	Anode: BDD; pH=3; V=50 ml; t=60 min; I=30 mA; U=5.8 V; V_{air}=100 mL/min;	3.75	348	(50 mg/L dimethyl phthalate) 93 %	6
$Fe^{II}Fe^{III}$ layered double hydroxide multiwall	Anode: Ti_4O_7 anode; pH=3; V_{air}=1 L/min; t=50 min; Current density=7.5 mA/cm^2;	52.0	-	(0.2 mM Sulfamethazine) 100 %	7
Fe^0-in-CNTs	Anode: DSA; V=300 ml t=60 min; V=300 ml; I=60 mA; V_{air}=0.4 L/min; t=120 min	(pH=3) 3.21	32.80	(50 mg/L phenol) 91.12 %	This work

		(50 mg/L phenol)	51.01
(pH=7) 1.67	26.05		
		%	

Table S2. Performance comparison of iron modified carbon materials with the literature.

-: not available

References:

1. D. Li, Y. Qu, J. Liu, W. He, H. Wang and Y. Feng, Y. *J. Power Sources*, 2014, **272**, 909-914.
2. X. Ding, S. Wang, W. Shen, Y. Mu, L. Wang, H. Chen and L. Zhang, *Water Res.*, 2017, **112**, 9-18.
3. X. Ding, Z. Ai and L. Zhang, *J. Hazard. Mater.,* 2012, **239**, 233-40.
4. Y. Zhang, M. Gao, S.-G. Wang, W. Zhou, Y. Sang and X.-H Wang, *Electrochim. Acta,* 2017, **231**, 694-704.
5. H. Zhao, Y. Chen, Q. Peng, Q. Wang and G. Zhao, *Appl. Catal. B,* 2017, **203**, 127-137.
6. H. Zhao, L. Qian, Y. Chen, Q. Wang and G. Zhao, *Chem. Eng. J.,* 2018, **332**, 486-498.
7. S. Ganiyu, T. Huong Le, M. Bechelany, N. Oturan, S. Papirio, G. Esposito, E. Hullebusch, M. Cretin and M. A. Oturan, *Chem. Eng. J.,* 2018, **350**, 844-855.